



Research article

Fatty acid composition in mammary adipose tissue measured by Gradient-echo Spectroscopic MRI and its association with breast cancers



Alana A. Lewin*, Pippa Storey, Melanie Moccaldi, Linda Moy, S. Gene Kim

New York University School of Medicine, Department of Radiology, Center for Biomedical Imaging, 660 First Avenue, 4th Floor, New York, NY 10016, United States

ARTICLE INFO

Keywords:

Fatty acid
Mammary adipose tissue
Gradient-echo spectroscopic MRI
Breast cancer
Postmenopausal

ABSTRACT

Purpose: To assess the association of fatty acid levels in mammary adipose tissue of postmenopausal women with the presence of breast cancer using the Gradient-echo Spectroscopic Imaging (GSI).

Materials and methods: Unilateral GSI was performed at 3 T in 61 postmenopausal women undergoing breast MRI exams. The study included 19 women with breast cancer, 23 women with benign/high risk lesions, and 19 women with a history of cancer. Voxel-wise spectral analysis of fatty acids was conducted to measure relative portions of monounsaturated (MUFA), polyunsaturated (PUFA), and saturated fatty acids (SFA) in each voxel. The voxels within mammary adipose tissue were automatically selected and their median fatty acid fractions were used for quantitative analysis. Statistical analyses were performed using χ^2 test, one-way analysis of variance (ANOVA) with Tukey-Kramer multiple comparison tests, and linear regression.

Results: Postmenopausal women with malignancies had significantly higher SFA (0.336 ± 0.038) in mammary adipose tissue compared to those with benign disease (0.283 ± 0.046 , $p = 0.0008$) and to those with a history of breast cancer (0.287 ± 0.050 , $p = 0.0038$). Postmenopausal women with malignant lesions had significantly lower MUFA (0.352 ± 0.041) compared to those with benign disease (0.401 ± 0.043 , $p = 0.0032$) and with history of breast cancer (0.388 ± 0.055 , $p = 0.0484$). The history of cancer group had a significant correlation ($r = 0.60$, $p = 0.006$) between SFA and BMI, and the cancer group had a significant correlation ($r = 0.57$, $p = 0.010$) between PUFA and BMI.

Conclusions: Fatty acid composition of mammary adipose tissue, particularly higher SFA and lower MUFA, may be associated with breast cancer. The GSI method utilizes an automated voxel-based analysis to measure fatty acid composition, and may be used to assess the role of mammary adipose tissue in cancer development and progress.

1. Introduction

Obesity is a well-known risk factor for numerous malignancies, including breast cancer. Obesity leads to changes in the production of steroid hormones and adipokines, as well as chronic inflammation, which have been implicated in carcinogenesis, tumor progression, and metastasis [1]. Obesity has been shown to cause chronic, subclinical inflammation as evidenced by elevated levels of circulating pro-inflammatory mediators [1]. The inflamed adipose tissue and circulating pro-inflammatory mediators favor tumor initiation and progression [2].

In postmenopausal women, body mass index (BMI) is an important risk factor for breast cancer development and invasiveness [3]. After menopause, there is a decrease in circulating estradiol levels and estrogen production occurs via the aromatization of androgens into estrogen in mammary adipose tissue, the principal source of estrogens

after menopause [4,5]. Menopause has also been shown to alter the amount and distribution of adipose tissue through the body [6]. As a result, there is an increased risk of developing breast cancer with increased BMI after menopause [7–11].

Recent studies also demonstrated that lipid composition distant from lesions is different depending on the malignancy of the lesion [12]. While MR-visible lipids in the tumor microenvironment have been studied extensively, the relationship between lipid composition in mammary adipose tissue and cancer development remains poorly understood. One of the challenges in investigating lipid composition of the breast in the clinical setting is the lack of rapid data acquisition methods that can cover a large portion of the breast with adequate spatial resolution for the complex structure of fibroglandular and mammary adipose tissue.

Recently, Gradient-echo Spectroscopic Imaging (GSI) has been

* Corresponding author.

E-mail address: Alana.Amarosa@nyumc.org (A.A. Lewin).

<https://doi.org/10.1016/j.ejrad.2019.04.024>

Received 5 February 2019; Received in revised form 4 April 2019; Accepted 29 April 2019

0720-048X/ © 2019 Elsevier B.V. All rights reserved.

introduced to measure fractions of different fatty acids, such as saturated fatty acid (SFA), monounsaturated fatty acid (MUFA), and polyunsaturated fatty acid (PUFA), in the mammary adipose tissue [9]. It can be easily conducted during diagnostic breast MRI exams with extra 5 min of acquisition time. The GSI method demonstrated that postmenopausal women with breast cancer have a significantly higher proportion of SFA in mammary adipose tissue than those with benign diseases [9]. However, the analysis was conducted based on the regions of interest (ROI) manually selected by two readers. Hence, the purpose of this study was to utilize GSI with an automated voxel-based analysis of fatty acid composition for assessment of the association of fatty acid levels in mammary adipose tissue of postmenopausal women with breast cancer.

2. Materials and methods

2.1. Patients

This retrospective study was Health Insurance Portability and Accountability.

Act compliant and was approved by our institutional review board. Informed consent was waived. Eighty-one postmenopausal women underwent a 5-minute examination of three-dimensional multiple gradient-echo sequence at the end of their diagnostic MRI examinations between July 2013 and November 2015. This includes 47 postmenopausal women who were part of an earlier study that investigated the lipid composition in both pre- and post-menopausal women [9]. Fourteen cases were technically unsuccessful, due to operator error ($n = 3$) or severe motion artifacts ($n = 11$), and were excluded from the final analysis. In addition, 6 cases of ductal carcinoma in situ (DCIS) were excluded from the study considering the uncertainty whether they would become invasive cancer. The final cohort included 61 postmenopausal women (mean age, 60.21 ± 8.17 years; age range, 47–81 years) (Fig. 1). Clinical indications for the MRI examinations include evaluation of extent of disease in the setting of known cancer, asymptomatic high-risk screening, further evaluation of imaging finding/problem solving, or annual surveillance after cancer. Patients with benign tissue (healthy tissue or benign lesions; $n = 23$), breast cancer ($n = 19$) and those with a history of breast cancer ($n = 19$) were included in the study. Of those cases with breast cancer, 17 were invasive

ductal carcinomas and 2 were invasive lobular carcinomas.

Information including patient age, clinical history, family history of breast cancer, BRCA mutation carrier, and MRI guided biopsy pathology were culled from the medical record. Table 1 is a summary of patient characteristics. Each patient's height and weight were measured at the time of the examination and were used to calculate their BMI. Mammographic breast density data were obtained from the mammographic reports and were confirmed by a fellowship-trained breast imaging radiologist (XX with 2 years of experience).

2.2. MRI data acquisition

The MRI scans were conducted using a whole body 3 T MRI system (Tim Trio; Siemens, Erlangen, Germany) and a dedicated seven-element bilateral breast coil (In vivo, Orlando, FL). All patients underwent a standard clinical diagnostic bilateral breast MRI exam that includes T1 and T2 weighted sequences followed by dynamic contrast-enhanced (DCE) MRI with an injection of gadobutrol (Gadavist; Bayer Healthcare, Whippany, NJ) at the standard dose of 0.1 mmol per kilogram of body weight. The GSI sequence was performed at the end of the clinical exam to acquire unilateral 3D MR images with voxel-by-voxel spectroscopic information. We assumed the effect of contrast injection on our measurement was close to negligible since the lipid spectrums were measured in the adipose tissue. This assumption is supported by a previous study demonstrating that the average line width of the methylene peak at 1.3 ppm was 13.9 ± 3.0 Hz when measured from the data acquired about 10 min after the contrast injection [9]. For GSI, a modified 3D gradient echo sequence was used to acquire 144 monopolar echoes with echo spacing = 1.44 ms and the following imaging parameters: TR = 220 ms, FA = 10° , spatial resolution = $2.8 \times 2.8 \times 2.8$ mm³, image matrix size = $96 \times 84 \times 18$, field of view = $270.0 \times 236.3 \times 50.4$ mm³, and scan time = 5 min. The sagittal imaging slab was positioned to cover one breast with a known or previously treated cancer if any; otherwise, the slab was positioned on a randomly selected side.

2.3. MRI data analysis

Voxel-wise spectral analysis of fatty acids was conducted by performing a Fourier transform of the complex-valued gradient-echo image data along the echo dimension, as shown in Fig. 2. After applying zero/first-order phase corrections, a spectral model consisted of 10 Voigt line profiles and a linear baseline was fit to the corrected spectral data. The parameters were estimated by minimizing the mean squared difference between the measured and predicted spectral data, using the Simplex method provided in IDL (Harris Geospatial Solutions, Broomfield, CO). The positions of Voigt profiles were initially set to literature values: 0.90, 1.30, 1.59, 2.03, 2.25, 2.77, 4.09, 4.28, 5.21, and 5.31 ppm [13]. The resonance areas of 10 lipid peaks (denoted as A to J in Fig. 2) were determined by integrating the estimated Voigt profiles. The spectral data analysis was conducted using a custom-written script in IDL. A voxel was considered a valid fat voxel if the line area of bulk CH₂ methylene protons at 1.3 ppm (denoted as B in Fig. 2) is the largest among the 10 line areas and the line area peak B is more than 40% and less than 60% of the sum of all line areas.

Among the 10 peaks of a valid fat voxel, we are interested in three resonances corresponding to allylic CH₂ protons, α - to a double bond, at 2.03 ppm (D), CH₂ methylene protons, α - to the carbonyl, at 2.25 ppm (E), and diallylic CH₂ protons at 2.77 ppm (F). These peaks and their combinations can be used to measure relative levels of MUFA, PUFA, and SFA (6, 7). Briefly, PUFA = area(F)/area(E), the ratio of the bridging diallylic protons to the methylene protons to COO in fatty acid chains; MUFA = $0.5 \text{ area(D)}/\text{area(E)}$ -PUFA, the relative area of allylic protons α to double bonds that are not part of multiple double bonds; SFA = $1 - \text{PUFA} - \text{MUFA}$. The color parameter maps in Fig. 2 show the fatty acid fractions estimated voxel-wise. The median value of all valid fat voxels was used as a representative value for each patient.

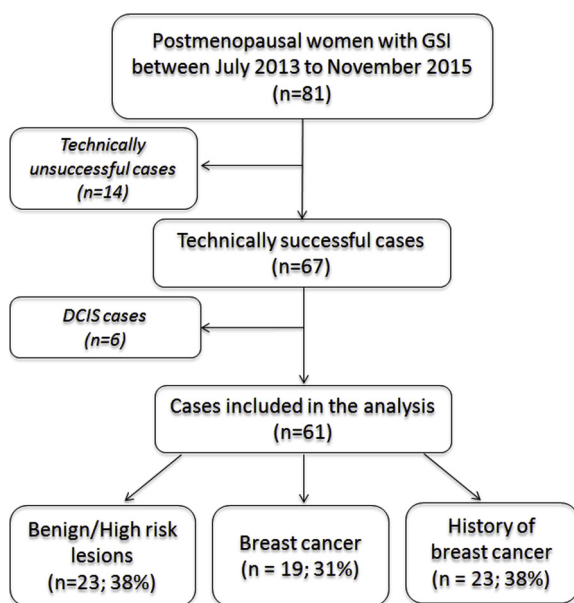


Fig. 1. Flow chart for selection of women who were included in the Gradient-echo Spectroscopic Imaging (GSI) study. Technically unsuccessful cases are due to operator errors ($n = 3$) and severe motion artifacts ($n = 11$).

Table 1
Patient information.

	Cancer (C)	Benign/High risk (B)	History of Cancer (H)	p-value		
				C vs B	C vs H	B vs H
N	19	23	19			
Age	61.6 ± 8.0	61.1 ± 8.7	57.7 ± 7.6	0.83	0.13	0.20
BMI	27.1 ± 4.8	25.0 ± 3.7	26.3 ± 4.7	0.13	0.61	0.33
Family history of breast cancer	7	16	14			
BRCA mutation carrier	1	11	3			
Clinical Indication						
1	16	0	0			
2	0	18	1			
3	2	4	3			
4	1	1	15			
BI-RADS						
1	0	9	0			
2	0	8	13			
3	0	1	5			
4	8	5	1			
5	2	0	0			
6	9	0	0			
BPE						
Minimal	10	12	13	0.23	0.36	0.29
Mild	6	11	6			
Moderate	1	0	0			
Marked	2	0	0			
FGT						
Almost entirely fat	1	3	1	0.39	0.99	0.51
Scattered fibroglandular	13	12	12			
Heterogeneous	4	8	5			
Extreme	1	0	1			
Mammographic Density						
Predominantly fatty	1	1	0	0.98	0.69	0.80
Scattered fibroglandular	11	13	10			
Heterogeneously dense	6	7	7			
Extremely dense	1	2	2			

*Clinical indication for study (1 = extent of disease; 2 = HR screening; 3 = further evaluation of imaging finding/problem solving; 4 = annual surveillance after cancer).

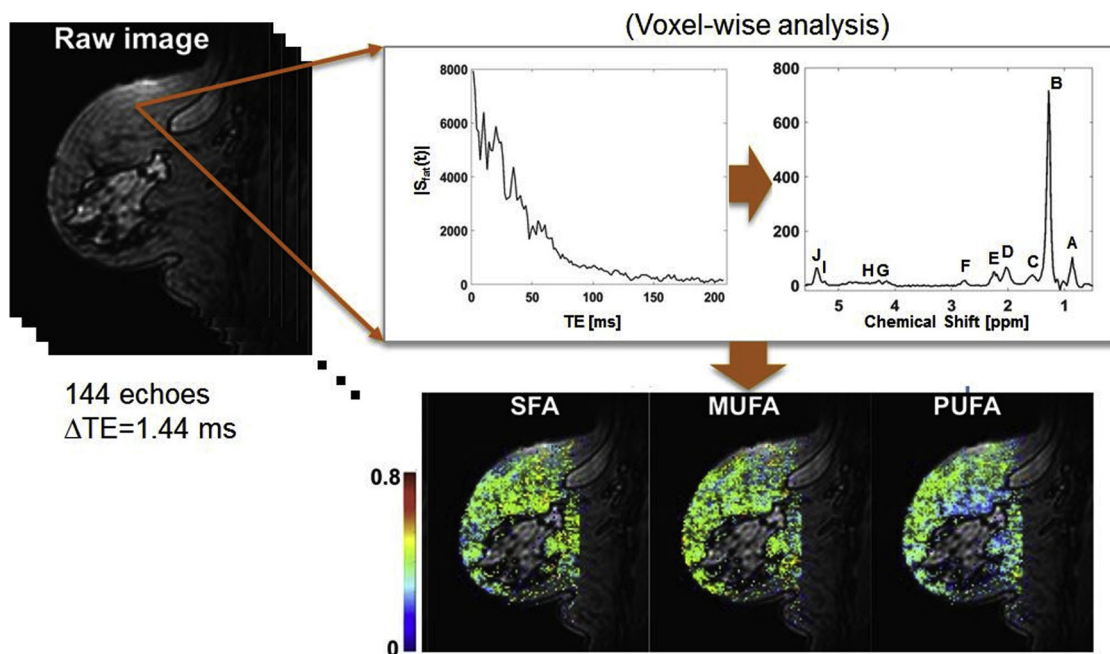


Fig. 2. Voxel-wise analysis of breast GSI data to generate parameter maps of saturated fatty acid (SFA), mono-unsaturated fatty acid (MUFA), and poly-unsaturated fatty acid (PUFA). The resonance areas of 10 lipid peaks (denoted as A to J) were determined by integrating the estimated Voigt profiles. A voxel was considered a valid fat voxel if the line area of bulk CH methylene protons at 1.3 ppm (B) is the largest among the 10 line areas and the line area peak B is more than 40% and less than 60% of the sum of all line areas.

Table 2
Comparison of fatty acid fractions among patients with benign, breast cancer, and history of cancer.

	Benign Mean ± SD	Cancer Mean ± SD	History Mean ± SD	One-way ANOVA		Tukey's multiple comparisons test					
				F	p-value	Benign vs Cancer		Benign vs History		Cancer vs History	
						Mean difference (95% CI)	p-value	Mean difference (95% CI)	p-value	Mean difference (95% CI)	p-value
SFA	0.283 ± 0.046	0.336 ± 0.038	0.287 ± 0.050	8.70	0.0005	−0.054 (−0.087, −0.020)	0.0008	−0.005 (−0.038, 0.029)	0.9409	0.049 (0.014, 0.084)	0.0038
MUFA	0.401 ± 0.043	0.352 ± 0.041	0.388 ± 0.055	6.15	0.0038	0.049 (0.015, 0.084)	0.0032	0.013 (−0.022, 0.047)	0.6435	−0.036 (−0.072, −0.000)	0.0484
PUFA	0.302 ± 0.039	0.298 ± 0.051	0.318 ± 0.046	1.02	0.3670	0.003 (−0.030, 0.037)	0.9734	−0.016 (−0.050, 0.017)	0.4826	−0.019 (−0.054, 0.016)	0.3910

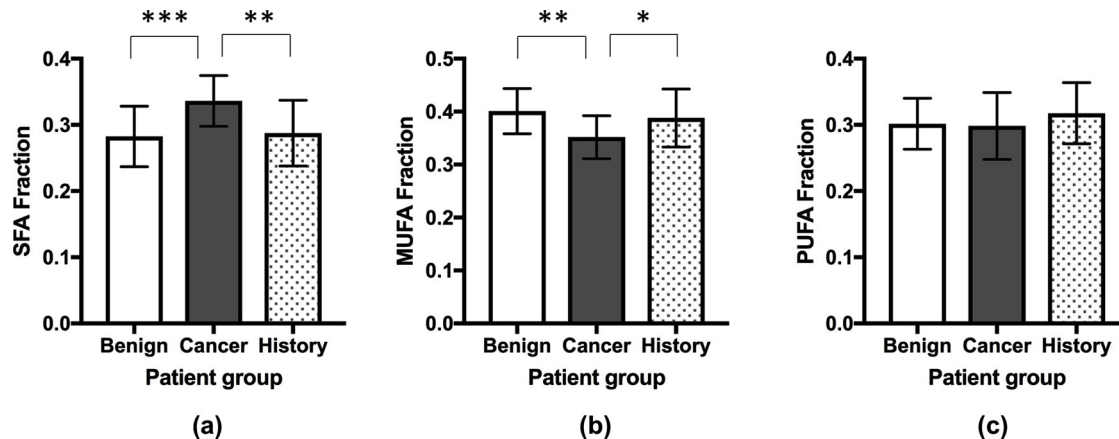


Fig. 3. Comparison among women with benign lesion, breast cancer, and a history of breast cancer in terms of saturated fatty acid (SFA) (a), monounsaturated fatty acid (MUFA) (b), and polyunsaturated fatty acid (PUFA) (c). * for $p < 0.05$, ** for $p < 0.01$, *** for $p < 0.001$.

The figure demonstrates that there was a statistically significant difference between the SFA values among the three groups (a). There was a statistically significant difference between the MUFA values among the three groups (b). No significant difference in PUFA was observed between the three cohorts (c).

The relative amount of fibroglandular tissue in the breast and background parenchymal enhancement (BPE) was assessed using the clinical MR images acquired in the same diagnostic exam. BPE was classified by using the Breast Imaging Reporting and Data System (BI-RADS) categories as none or minimal, mild, moderate, or marked [14]. Fibroglandular tissue was also classified by using BI-RADS categories as almost entirely fat, scattered, heterogeneous, and extreme fibroglandular tissue [15]. BPE and fibroglandular tissue data were obtained from the MRI reports and were confirmed by a fellowship-trained breast imaging radiologist (XX with 2 years of experience).

2.4. Statistical analyses

The χ^2 test was used for comparison between patient groups in terms of the categorical measures of conventional breast imaging characteristics, such as BPE, fibroglandular tissue and mammographic density. The t -test was used for other continuous variables. The fatty acid fractions measured for three patient groups (cancer, benign/high risk and history of cancer) were compared using the ordinary one-way analysis of variance (ANOVA) with Tukey-Kramer multiple comparison tests. Linear regression analysis was used to assess the association of fatty acid fractions with age and BMI. All statistical tests were conducted at the two-sided 5% significance level using GraphPad (GraphPad Software, Inc., CA).

3. Results

In our study, 19 women (61.6 ± 8.0 years) had a biopsy-proven invasive cancer, 23 women (61.1 ± 8.7 years) had biopsy-proven benign/high risk lesions, and 19 women (57.7 ± 7.6 years) had a history

of cancer. Of the 19 women with biopsy-proven malignancy, there were 17 invasive ductal carcinomas and 2 invasive lobular carcinomas. The malignant lesions were characterized as masses ($n = 11$), nonmass enhancement ($n = 4$), and both ($n = 4$). In addition, 17 of 19 breast cancers were located at the interface between mammary adipose tissue and fibroglandular tissue. The other 2/19 malignant lesions were found within central fibroglandular tissue and a recurrent chest wall tumor in the mastectomy bed, respectively. There was no statistically significant difference between the three cohorts in terms of age, BMI, BPE, fibroglandular tissue, or mammographic density (see Table 1).

A comparison of fatty acid fractions between the postmenopausal cohorts was performed as summarized in Table 2 and Fig. 3. There was a statistically significant difference between the SFA values among the three groups (ANOVA, $p = 0.0005$). The post hoc analysis showed that postmenopausal women with malignant lesions (0.336 ± 0.038) had significantly higher SFA compared to those with benign disease (0.283 ± 0.046 , $p = 0.0008$) and to those with a history of breast cancer (0.287 ± 0.050 , $p = 0.0038$). A statistically significant difference was also found between the MUFA values (ANOVA, $p = 0.0038$). The post hoc analysis showed that postmenopausal women with malignant lesions (0.352 ± 0.041) had significantly lower MUFA compared to those with benign disease (0.401 ± 0.043 , $p = 0.0032$) and with a history of breast cancer (0.388 ± 0.055 , $p = 0.0484$). No significant difference in PUFA was observed between the three cohorts ($p = 0.3670$).

Representative examples of fatty acid maps of women with benign or no suspicious lesion are shown in Fig. 4. It can be noted that the fatty acid fractions are distributed homogeneously across the breast parenchyma, although the spectral analysis was performed for individual voxels independently. Another example shown in Fig. 4 is for two

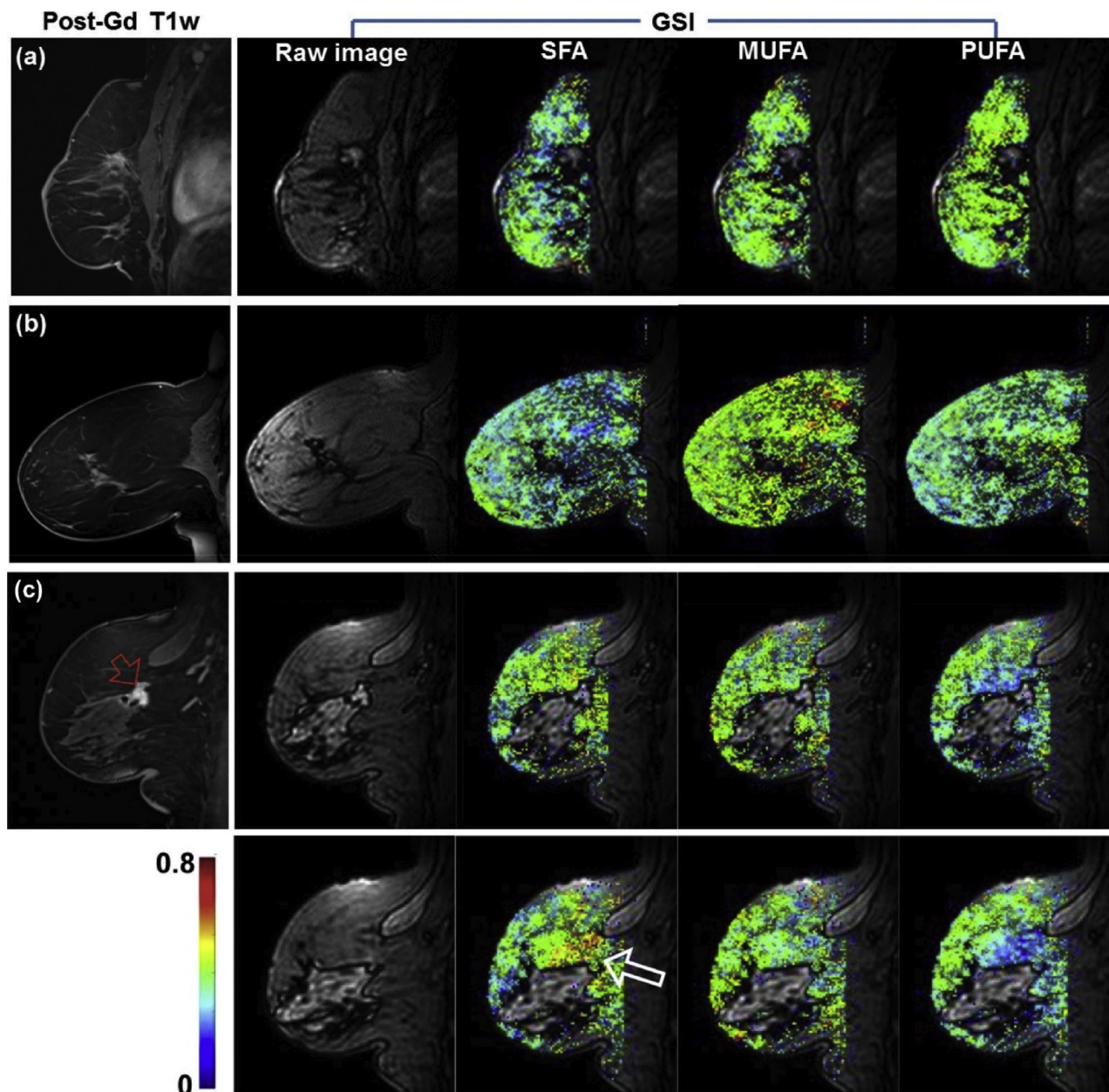


Fig. 4. Representative examples of fatty acid maps along with the raw images at first echo time of the GSI and post-Gd T1 weighted image. (a) A 66-year-old woman with post-surgical change. (b) A 59-year-old woman without any suspicious lesion. (c) A 67-year-old woman with newly diagnosed invasive ductal carcinoma (red arrow). The larger arrow (white) on the saturated fatty acid (SFA) map indicates higher level of SFA close to the lesion.

consecutive slices in a woman with invasive ductal carcinoma. It shows that the fatty acid fractions in two slices are similar to each other. The SFA close to the lesion appears to be higher than in the mammary adipose tissue away from the lesion. This was observed in this example and other cases. However, assessment of the local variability in the fatty acid fractions was beyond the scope of this study.

Fig. 5 shows linear regression between fatty acid fractions and age. There was no significant association of any fatty acid fraction with age in any group. A similar regression analysis with BMI (Fig. 5) showed that the history of cancer group had a significant correlation (Pearson correlation coefficient $r = 0.60$, $p = 0.006$) between SFA and BMI, and the cancer group had a significant correlation ($r = 0.57$, $p = 0.010$) between PUFA and BMI.

4. Discussion

In this study, GSI was used to conduct voxel-wise analysis of fatty acid composition in mammary adipose tissue of postmenopausal women. In comparison to a previous study based on manually selected regions of interest [9], our analysis of fatty acid composition was performed without the interaction with a reader to select ROIs for the mammary adipose tissue, such that this tool may be incorporated into the clinical workflow. By using this method, we found that SFA was significantly higher and MUFA was significantly lower in postmenopausal women with malignant tumors than in those with benign/high risk lesions and those with a history of breast cancer. These results are consistent with a previous study based on manually selected ROIs [9] and demonstrate that the same results, in terms of SFA and MUFA in postmenopausal women, can be observed when the measurement was conducted with all the voxels in the mammary adipose tissue

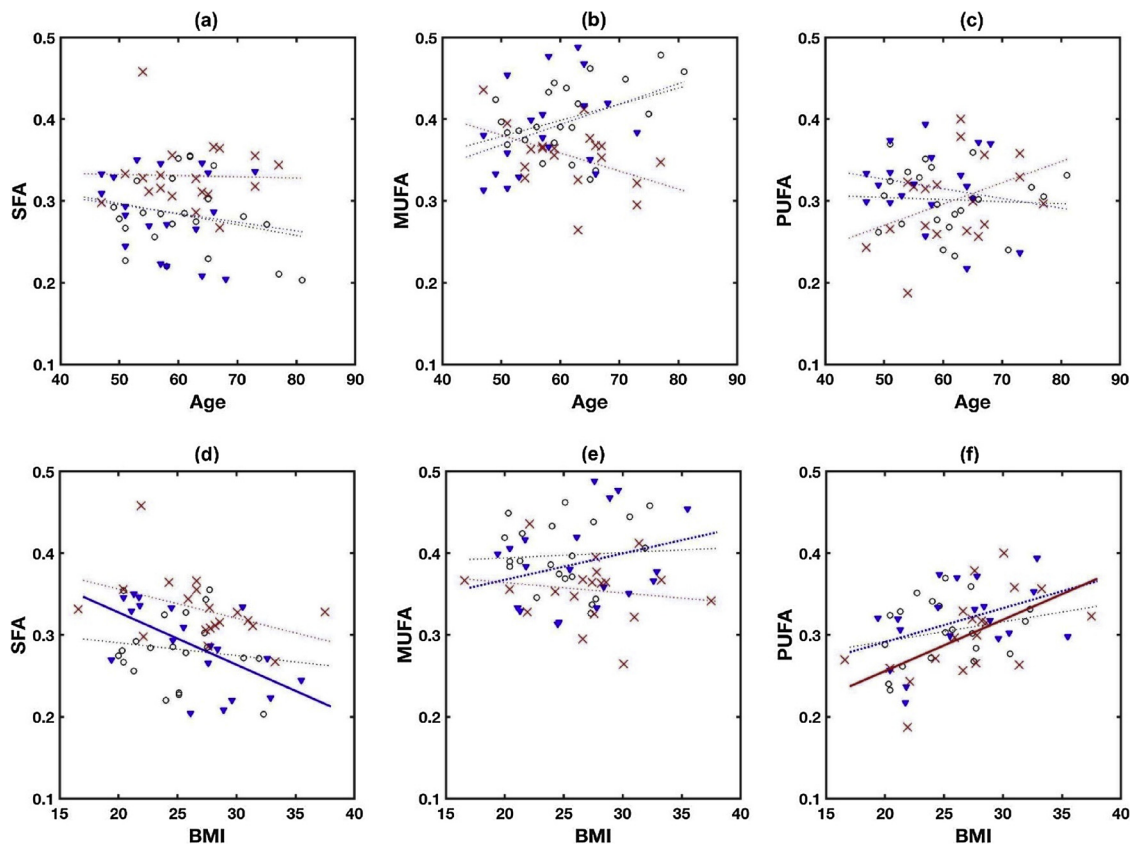


Fig. 5. Scatter plots of age with SFA (a), MUFA (b), and PUFA (c), and BMI with SFA (d), MUFA (b), and PUFA (f). Red crosses are for women with breast cancer, black circles for women with benign findings, and blue triangles for women with a history of breast cancer. Dotted lines are linear regression fits to the data in individual groups. There was no significant correlation between age and any of fatty acid fractions in any group. Solid lines are with statistical significance; $r = 0.60$ ($p = 0.006$) for SFA and BMI in women with a history of breast cancer, and $r = 0.57$ ($p = 0.01$) for PUFA and BMI in women with cancer.

automatically selected. The results from these two studies suggest that for post-menopausal women, high SFA and low MUFA may be associated with breast cancer development.

Few studies have used direct methods to assess how fatty acid fractions correlate with breast cancer. The results of several studies are consistent with those of our investigation. A study by Mamalakis et al. evaluated fatty acids by gas chromatography in gluteal adipose tissue of breast cancer patients and demonstrated lower MUFA and higher levels of a specific SFA in gluteal adipose tissue compared to healthy controls [16]. An epidemiologic study by Lof et al. also showed similar findings with respect to MUFA and breast cancer risk [17]. Freed et al. used an *in vivo* method to measure fatty acid fractions of mammary adipose tissue during diagnostic breast MRI and demonstrated high SFA and low MUFA levels in postmenopausal women with invasive cancer [9].

However, there are conflicting results reported in the literature. Victor et al. estimated fatty acid composition in more than 50 *ex vivo* breast samples by using carbon-13 MR spectroscopy for patients with cancer and healthy patients. They found no significant difference between the MUFA, PUFA, or SFA of mammary adipose tissue in cancer versus healthy patients; yet, they did find that cancer tissue had lower MUFA and higher SFA than noncancerous tissue [18]. In a case control study, Petrek et al. evaluated the relationship between breast cancer and fatty acid composition in *ex-vivo* breast and abdominal tissue samples in 154 women with invasive breast cancer and 125 women with benign tissue. No significant difference was observed in the fat composition between these two groups, even when grouped by menopausal status [19]. Hence, further studies with large cohorts are required to fully address the role of lipid composition in breast cancer development and progress. The present study demonstrates that the GSI method can be a useful non-invasive imaging tool to conduct a study

with a larger cohort with a relatively short scan time of 5 min.

In a long-term prospective study by Iyengar et al., relatively high body fat levels were associated with an elevated risk of invasive breast cancer in postmenopausal women with normal BMI [20]. Specifically, the study found a 56% increase in the risk of developing ER-positive breast cancer per 5-kg increase in trunk fat, despite a normal BMI [20]. The findings may be explained by the observations that enlarged adipocytes and inflammation are found in the breast tissue of some women with normal BMI [21]. Inflammation of breast white adipose tissue is seen in women with elevated levels of total body fat [22]. Inflamed breast white adipose tissue is associated with elevated levels of aromatase [23]. Specifically, high concentrations of aromatase, an enzyme that converts androgens to estrogen, have been shown in women with higher body fat [24]. Higher circulating levels of estradiol affect cell proliferation and breast cancer development through receptor dependent mechanisms as well as through receptor independent mechanisms via alterations in DNA [24]. Studies have also shown that reduction in dietary fat intake is associated with decrease in circulating serum estradiol levels [24,25]. The fatty acid composition of mammary adipose tissue may reflect dietary intake of the preceding 2–3 years, as opposed to hours to weeks [16,19]. It has been shown that both SFA and MUFA are produced in the human body and are not well correlated with dietary fat intake [26,27]. In contrast, PUFA cannot be produced endogenously; the tissue concentration of these dietary fats reflects a balance between dietary intake, metabolism, and storage [18,26]. In dietary intake animal studies assessing the effects of different fatty acids on mammary tumors, PUFA has been shown to correlate more strongly with cancer development than SFA or MUFA [28]. A meta-analysis by Fay et al. demonstrated that the tumor-enhancing effect of SFA is less than PUFA, but more than nonfat calories [28]. A systematic review

suggested that higher fat intake, specifically PUFA, is associated with increased risk of breast cancer [24]. The discrepancy between dietary fat intake studies and our analysis suggests that there is a different inherent biologic process affecting breast cancer development.

The hormonal level in mammary adipose tissue may directly affect the fibroglandular tissue in which mammary adipose tissue is embedded, as substantiated by recent studies showing a majority of breast cancers are found at the interface between mammary adipose tissue and fibroglandular tissue [29,30]. Understanding adipose tissue invasion may be an important tool for risk stratification of early dissemination of breast cancer. In most patients with breast cancer, only fibroglandular or fibroadipose tissue invasion by cancer cells appears insufficient for lymph node metastases [29]. Aromatase activity and adipocytokines in mammary adipose tissue may participate in adipose tissue invasion and its metastasis to lymph nodes [29]. Aromatase activity and expression have been shown to be most pronounced proximal to the malignant lesion in breast cancer [31,32]. In the study by Yamaguchi et al. [29], patients with adipose tissue invasion disease were significantly older. However, there was no significant association of BMI with adipose tissue invasion, suggesting that adipose tissue invasion may be affected by age-related increase in fat cells in the breast rather than the amount of whole body adipose tissue. Future studies are warranted to investigate whether the lipid composition measured by the GSI method is associated with the hormonal level in mammary adipose tissue and the subsequent association of the lipid composition of mammary adipose tissue with adipose tissue invasion.

Limitations of this study include a small sample size. All patients included in this study were patients who underwent diagnostic MR imaging for various clinical indications including asymptomatic high-risk screening. Hence, the benign group may represent patient populations at high risk for breast cancer. Future studies will include patients at normal risk. Another limitation of our study was that the data analysis was based on the median values of fatty acids fractions of individual patients and did not include the information regarding the spatial distribution of the lipid composition as it was beyond the scope of this study. In several cases including one shown in Fig. 4, we observed the SFA level is higher close to the invasive cancer. It cannot be determined from our study whether the locally elevated SFA is a cause or effect of the breast cancer. Further study is warranted to investigate the spatial distribution of fatty acids with respect to the location of breast cancer. In addition, further investigation of whether the lipid composition of mammary adipose tissue has a stronger or weaker association with any molecular subtypes of breast cancer could be explored.

In conclusion, we performed a GSI study combined with spatial mapping of fatty acid composition in postmenopausal women with and without malignant lesions. The results suggest that the lipid composition of the mammary adipose tissue, particularly higher SFA and lower MUFA, may be associated with the presence of breast cancer. The proposed GSI method does not require manually drawn ROIs for adipose tissue and utilizes all voxels in the adipose tissue automatically. This tool may be more easily incorporated into the clinical workflow during standard clinical diagnostic imaging sessions as well as in future studies with large cohorts, such that it can be used to investigate a possible association of fatty acid composition with other breast cancer risk factors, such as background parenchymal enhancement and breast density. While the role of dietary fat in human breast cancer remains unresolved, non-invasive in vivo evaluation of lipid composition of mammary adipose tissue using GSI may aid in breast cancer risk assessment and provide insight into physiological mechanisms that facilitate cancer development.

Conflict of interest

No conflicts of interest to disclose.

Funding from grants

R01CA219964, R01CA160620, P41EB017183.

References

- [1] N.M. Iyengar, C.A. Hudis, A.J. Dannenberg, Obesity and cancer: local and systemic mechanisms, *Annu. Rev. Med.* 66 (2015) 297–309.
- [2] W. Zhu, et al., Invasive breast cancer preferably and predominantly occurs at the interface between fibroglandular and adipose tissue, *Clin. Breast Cancer* 17 (1) (2017) e11–e18.
- [3] M. Wiseman, The second World Cancer Research Fund/American Institute for Cancer Research expert report, Food, nutrition, physical activity, and the prevention of cancer: a global perspective, *Proc. Nutr. Soc.* 67 (3) (2008) 253–256.
- [4] K.M. Nieman, et al., Adipose tissue and adipocytes support tumorigenesis and metastasis, *Biochim. Biophys. Acta* 1831 (10) (2013) 1533–1541.
- [5] H. Savolainen-Peltonen, et al., Breast adipose tissue estrogen metabolism in postmenopausal women with or without breast cancer, *J. Clin. Endocrinol. Metab.* 99 (12) (2014) E2661–7.
- [6] A. Meseguer, C. Puche, A. Cabero, Sex steroid biosynthesis in white adipose tissue, *Horm. Metab. Res.* 34 (11–12) (2002) 731–736.
- [7] K. Bhaskaran, et al., Body-mass index and risk of 22 specific cancers: a population-based cohort study of 5.24 million UK adults, *Lancet* 384 (9945) (2014) 755–765.
- [8] E.E. Calle, et al., Overweight, obesity, and mortality from cancer in a prospectively studied cohort of U.S. adults, *N. Engl. J. Med.* 348 (17) (2003) 1625–1638.
- [9] M. Freed, et al., Evaluation of breast lipid composition in patients with benign tissue and cancer by using multiple gradient-echo MR imaging, *Radiology* 281 (1) (2016) 43–53.
- [10] G.K. Reeves, et al., Cancer incidence and mortality in relation to body mass index in the Million Women Study: cohort study, *BMJ* 335 (7630) (2007) 1134.
- [11] A.G. Renehan, et al., Body-mass index and incidence of cancer: a systematic review and meta-analysis of prospective observational studies, *Lancet* 371 (9612) (2008) 569–578.
- [12] Q. He, et al., In vivo MR spectroscopic imaging of polyunsaturated fatty acids (PUFA) in healthy and cancerous breast tissues by selective multiple-quantum coherence transfer (Sel-MQC): a preliminary study, *Magn. Reson. Med.* 58 (6) (2007) 1079–1085.
- [13] J. Ren, et al., Composition of adipose tissue and marrow fat in humans by 1H NMR at 7 Tesla, *J. Lipid Res.* 49 (9) (2008) 2055–2062.
- [14] E.A. Morris, C.C. Lee, et al., ACR BI-RADS® magnetic resonance imaging, ACR BI-RADS® Atlas, Breast Imaging Reporting and Data System, American College of Radiology, Reston, VA, 2013.
- [15] E. Sickles, C.J. D'Orsi, L.W. Bassett, et al., ACR BI-RADS® mammography, ACR BI-RADS® Atlas, Breast Imaging Reporting and Data System, American College of Radiology, Reston, VA, 2013.
- [16] G. Mamlakis, et al., Adipose tissue fatty acids in breast cancer patients versus healthy control women from Crete, *Ann. Nutr. Metab.* 54 (4) (2009) 275–282.
- [17] M. Lof, et al., Dietary fat and breast cancer risk in the Swedish women's lifestyle and health cohort, *Br. J. Cancer* 97 (11) (2007) 1570–1576.
- [18] T.A. Victor, A. Bergman, R.H. Knop, Detecting fatty acids of dietary origin in normal and cancerous human breast tissue by 13C nuclear magnetic resonance spectroscopy, *Br. J. Cancer* 68 (2) (1993) 336–341.
- [19] J.A. Petrek, et al., Breast cancer risk and fatty acids in the breast and abdominal adipose tissues, *J. Natl. Cancer Inst.* 86 (1) (1994) 53–56.
- [20] N.M. Iyengar, et al., Association of body fat and risk of breast cancer in postmenopausal women with normal body mass index: a secondary analysis of a randomized clinical trial and observational study, *JAMA Oncol.* 5 (2) (2019) 155–163.
- [21] N.M. Iyengar, et al., Metabolic obesity, adipose inflammation and elevated breast aromatase in women with normal body mass index, *Cancer Prev. Res. (Phila)* 10 (4) (2017) 235–243.
- [22] C. Vayssie, et al., Inflammation of mammary adipose tissue occurs in overweight and obese patients exhibiting early-stage breast cancer, *NPJ Breast Cancer* 3 (2017) 19.
- [23] P.G. Morris, et al., Inflammation and increased aromatase expression occur in the breast tissue of obese women with breast cancer, *Cancer Prev. Res. (Phila)* 4 (7) (2011) 1021–1029.
- [24] L.B. Turner, A meta-analysis of fat intake, reproduction, and breast cancer risk: an evolutionary perspective, *Am. J. Hum. Biol.* 23 (5) (2011) 601–608.
- [25] L. Hilakivi-Clarke, et al., Do estrogens always increase breast cancer risk? *J. Steroid Biochem. Mol. Biol.* 80 (2) (2002) 163–174.
- [26] L. Arab, Biomarkers of fat and fatty acid intake, *J. Nutr.* 133 (Suppl. 3) (2003) 925S–932S (3).
- [27] S.J. London, et al., Fatty acid composition of subcutaneous adipose tissue and diet in postmenopausal US women, *Am. J. Clin. Nutr.* 54 (2) (1991) 340–345.
- [28] M.P. Fay, et al., Effect of different types and amounts of fat on the development of mammary tumors in rodents: a review, *Cancer Res.* 57 (18) (1997) 3979–3988.
- [29] J. Yamaguchi, et al., Prognostic impact of marginal adipose tissue invasion in ductal carcinoma of the breast, *Am. J. Clin. Pathol.* 130 (3) (2008) 382–388.
- [30] W. Zhu, et al., Invasive breast cancer preferably and predominantly occurs at the interface between fibroglandular and adipose tissue, *Clin. Breast Cancer* 17 (1) (2017) e11–e18.
- [31] J.S. O'Neill, R.A. Elton, W.R. Miller, Aromatase activity in adipose tissue from breast quadrants: a link with tumour site, *Br. Med. J. (Clin. Res. Ed.)* 296 (6624) (1988) 741–743.
- [32] H. Sasano, M. Ozaki, Aromatase expression and its localization in human breast cancer, *J. Steroid Biochem. Mol. Biol.* 61 (3–6) (1997) 293–298.